Enzyme Catalysis

International Edition: DOI: 10.1002/anie.201908535
German Edition: DOI: 10.1002/ange.201908535

Low-Barrier and Canonical Hydrogen Bonds Modulate Activity and Specificity of a Catalytic Triad

Prashasti Kumar, Pratul K. Agarwal, M. Brett Waddell, Tanja Mittag, Engin H. Serpersu, and Matthew J. Cuneo**

Dedicated to Elizabeth E. Howell

Abstract: *The position, bonding and dynamics of hydrogen atoms in the catalytic centers of proteins are essential for catalysis. The role of short hydrogen bonds in catalysis has remained highly debated and led to establishment of several distinctive geometrical arrangements of hydrogen atoms vis-à-vis the heavier donor and acceptor counterparts, that is, low-barrier, single-well or short canonical hydrogen bonds. Here we demonstrate how the position of a hydrogen atom in the catalytic triad of an aminoglycoside inactivating enzyme leads to a thirty-fold increase in catalytic turnover. A low-barrier hydrogen bond is present in the enzyme active site for the substrates that are turned over the best, whereas a canonical hydrogen bond is found with the least preferred substrate. This is the first comparison of these hydrogen bonds involving an identical catalytic network, while directly demonstrating how active site electrostatics adapt to the electronic nature of substrates to tune catalysis.*

Introduction

Enzyme active sites inherently encode some level of plasticity as they must be able to accommodate diverse substrates, stabilize/destabilize intermediates, and release products within the confines of a restricted space.[1] The response of an enzyme to substrate molecules at different stages of the reaction coordinate ultimately tunes catalytic rate constants and specificity profiles. Molecular recognition and the response of substrates and reaction intermediates to the local electrostatic environment of the enzyme's reaction center is defined by dissociation constants (pK_a) of the active site residues, which play important roles in the ability to turn over and catalytically differentiate amongst related substrates.[2]

Matched pK_a values for the heavy atom donors and acceptors are central to the low-barrier hydrogen bond (LBHB) hypothesis first proposed in the early 1990s.[3] The hallmark of an LBHB is that they are short hydrogen bonds ($\approx$2.65 Å for nitrogen and oxygen heavy atoms) in which the matched pKa values of heavy atom donor (N) and acceptor (O) groups lead to the proton residing equidistant between these atoms.[4] Due to the nature of this strong hydrogen bond, LBHBs have been proposed to be responsible for the catalytic efficiencies of several enzymes including citrate synthase,[5] serine proteases,[6] ketosteroid isomerase,[7] aspartate aminotransferase,[8] amongst several others. However, the specific role of LBHBs in enzyme catalysis remains debated[9] as direct evidence for LBHB-mediated enhancement of catalysis is lacking. Moreover, the precise location of a single hydrogen atom can be experimentally difficult to determine and many structural and biochemical studies of enzymes have relied upon neighboring heavy atom distances to predict the position of a hydrogen atom involved in an LBHB.[10] Discrepancies among studies of LBHBs,[11] coupled to the finding of short canonical hydrogen bonds, or short ionic hydrogen bonds (SIHBs), in place of where LBHBs were predicted[12] has led to the contentious nature of the proposed role of LBHBs in catalysis.

Recently, an LBHB was discovered in the non-canonical catalytic triad (Glu192–His189–antibiotic amine) of the aminoglycoside-*N3*-acetyltransferase VIa (AAC-VIa) using neutron diffraction,[13] and was proposed to play a key role in enzyme catalysis (Figure 1). Similar to other aminoglycoside acetyltransferases, AAC-VIa uses acetyl coenzyme A (acetyl CoASH) as an acetyl donor,[14] but unlike them it has a narrow substrate specificity profile. AAC-VIa recognizes a set of highly similar antibiotics, but modifies them with catalytic efficiencies that vary 30-fold[15] (Figure 1). These previous kinetic studies determined gentamicin to be the most preferred substrate, followed by sisomicin, both of which are structurally identical except for a double bond in the

[*] Dr. P. Kumar
Graduate School of Genome Science and Technology, University of Tennessee, Knoxville, TN, 37996 (USA)
and
Present address: Department of Pharmacological Sciences, Icahn School of Medicine at Mount Sinai, New York, NY, 10029 (USA)
Dr. P. K. Agarwal, Dr. E. H. Serpersu
Department of Biochemistry and Cellular and Molecular Biology, University of Tennessee, Knoxville, TN, 37996 (USA)
M. B. Waddell
Molecular Interaction Analysis Shared Resource, St. Jude Children's Research Hospital
Memphis, TN, 38105 (USA)
Dr. T. Mittag, Dr. M. J. Cuneo
Department of Structural Biology, St. Jude Children's Research Hospital, Memphis, TN, 38105 (USA)
Dr. E. H. Serpersu
National Science Foundation, Alexandria, VA, 22314 (USA)
E-mail: eserpers@nsf.gov
Dr. M. J. Cuneo
Oak Ridge National Laboratory, Oak Ridge, TN, 37830 (USA)
E-mail: matt.cuneo@stjude.org
Supporting information and the ORCID identification number(s) for the author(s) of this article can be found under https://doi.org/10.1002/anie.201908535.

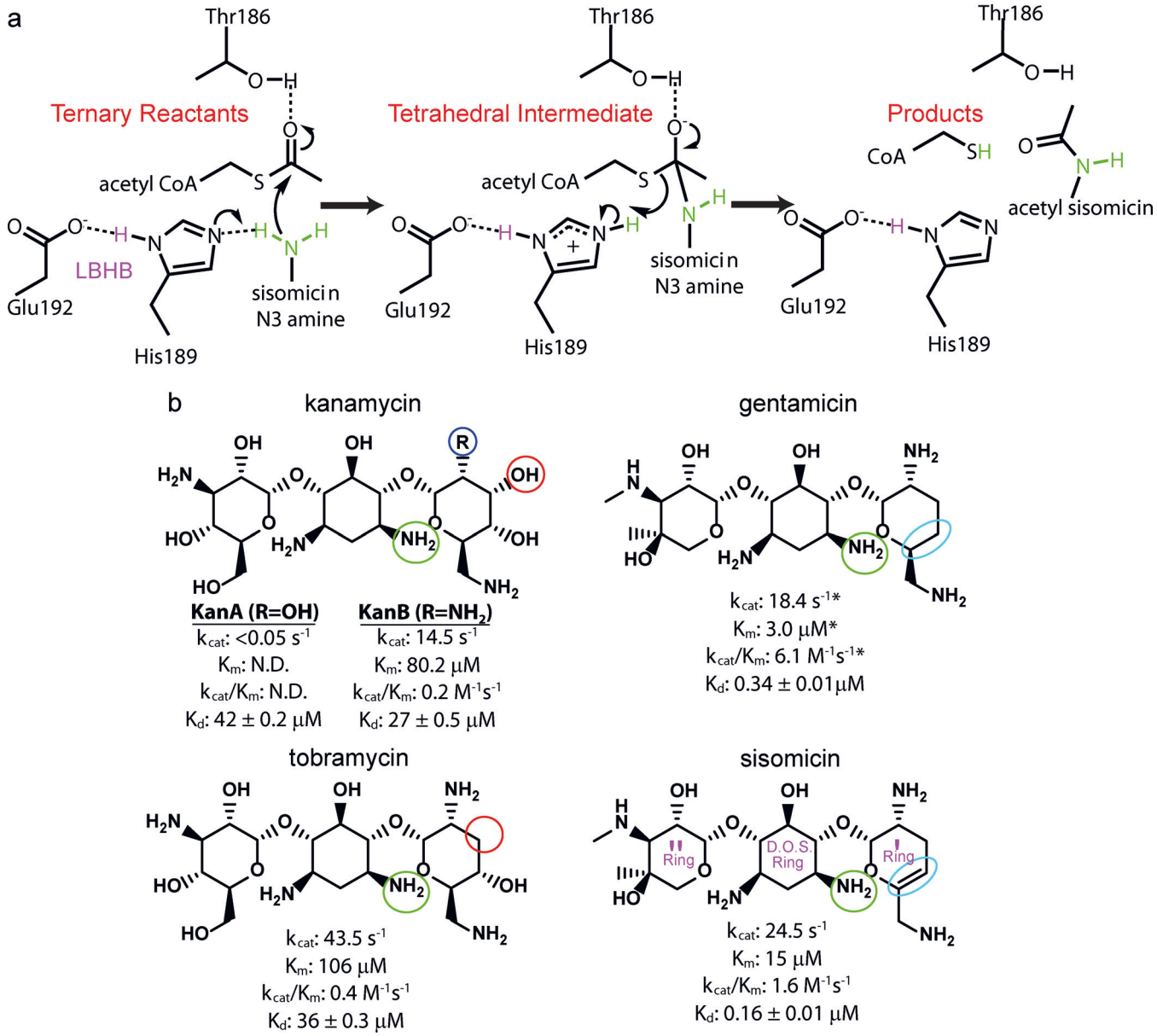

Figure 1. Aminoglycoside antibiotic substrates and mechanism of AAC-VIa. a) The proposed catalytic mechanism of AAC-VIa. The non-canonical AAC-VIa catalytic triad consists of Glu192, His189 and the N3 amine of the antibiotic substrates (green atom labels). The hydrogen atom which was found to be in an LBHB in the presence of sisomicin is colored magenta. b) The antibiotic substrates of AAC-VIa used in this study, as well as the previously determined[15] kinetic parameters and the SPR-based K_d values determined in this study are shown. The single difference between kanamycins and tobramycin is circled in red, and the substituent group which is an amine in kanamycin B and a hydroxyl in kanamycin A is circled in blue. The K_m values were not determined (N.D.) for kanamycin A. The single bond difference between gentamicin and sisomicin is circled in cyan. The site of AAC-VIa mediated acetylation is circled in green. Sisomicin is labeled (magenta text) based on the aminoglycoside nomenclature for the three rings. The central ring of the aminoglycoside is the 2-deoxystreptamine core (DOS Ring), the ring to the left of the core is the double primed ring (″) and the ring to the right is the primed ring (′). *Kinetic parameters were determined for gentamicin C2, which has a methyl group and a primary amine on the C6 carbon. Gentamicin C1a, which lacks this methyl was used in this study.

primed ring of sisomicin (Figure 1). Among aminoglycosides that can be modified by AAC-VIa, kanamycin B is the least preferred substrate. Interestingly, kanamycin A differs from kanamycin B by just a single amine versus a hydroxyl group substitution at the C2′ position on the antibiotic and is not modified by AAC-VIa (Figure 1).

Here we use complementary X-ray and neutron crystallographic structure determination of a series of similar aminoglycosides bound to AAC-VIa to understand the underlying molecular basis for the observed specificity profile of this enzyme. These studies on AAC-VIa clearly show the presence of a hydrogen atom involved in an LBHB in the catalytic triad of the best turned over ligands, yet in the structure of the substrate which is turned over the poorest a canonical hydrogen bond is found. Since hydrogen atoms can scatter neutrons strongly,[16] an LBHB is clearly visible in the catalytic

triad of AAC-VIa in the case of those ligands with the best catalytic efficiency, with a proton residing equidistant between the donor and acceptor atoms. In the case of the poorest substrate, a canonical hydrogen bond is observed, with the proton bound to the nitrogen atom of His189. These structures demonstrate how the local electrostatic environment of the enzyme active site responds to different chemical substituents on the substrate and tunes catalytic activity through modulating the strength of the catalytic hydrogen bond, while also shedding light on the molecular principles underlying ligand selection by enzymes in general.

Results

Interaction of antibiotics with AAC-VIa

The kinetic parameters of AAC-VIa with the five antibiotics used in this study were previously determined and showed that the catalytic efficiency profile was gentamicin ≈ sisomicin > tobramycin > kanamycin B ⩾ kanamycin A.[15] In what was largely a K_m effect, these substrates were turned over with an overall 30-fold difference in catalytic efficiency (Figure 1). Here we support these earlier kinetic results using surface plasmon resonance (SPR) measurements of substrates binding to AAC-VIa in the absence of the acetyl-CoASH acetyl donor molecule, although previous work has shown that antibiotics bind tighter in the presence of the cofactor product.[15] In the absence of coenzyme A, sisomicin and gentamicin had essentially identical dissociation constants (K_d), whereas tobramycin, kanamycin A and kanamycin B had essentially identical K_d values relative to each other, yet approximately two orders of magnitude weaker than those for gentamicin and sisomicin (Figure 1 and Figure S1). The identical binding constants of kanamycin A and B are surprising as no turnover of kanamycin A was detected in kinetic assays. This suggests something other than direct molecular recognition of substrates determines the kinetic distinction between different aminoglycosides by AAC-VIa.

Structural studies of aminoglycosides bound to AAC-VIa

To understand the underlying structural basis of the antibiotic substrate profile of AAC-VIa, the crystal structures of the complexes of AAC-VIa with sisomicin, gentamicin C1a, tobramycin, kanamycin B and kanamycin A were determined to high-resolution (1.14–1.39 Å resolution) (Table S1 and Figure S2). Additionally, the apo structure of AAC-VIa was determined to a resolution of 1.60 Å (Table S1). The structures of the apo and sisomicin-bound AAC-VIa were determined previously, yet at a significantly lower resolution.[13]

Although AAC-VIa kinetically discriminates among these five antibiotics, the X-ray crystallographic structures are all highly similar (Figure 2 and Figure S3). Indeed, the hydrogen bonding pattern and network of binding site water molecules are essentially identical, with the largest differences occurring in the primed ring of the aminoglycosides. In

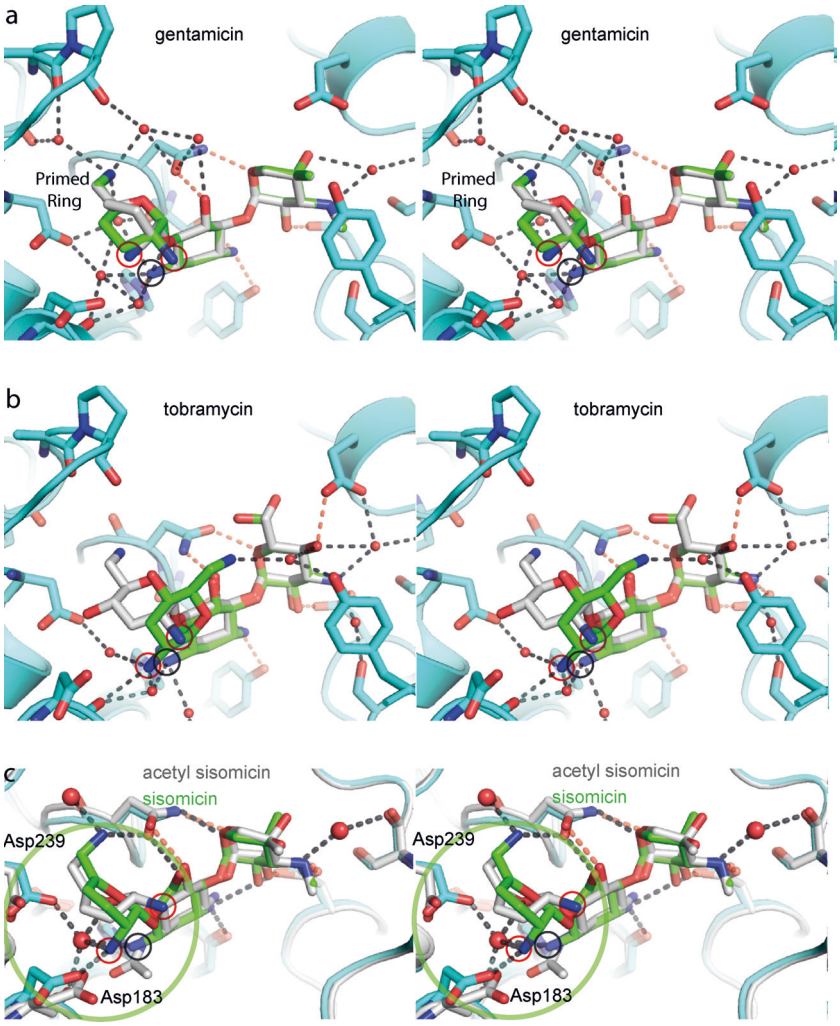

Figure 2. Ligand conformers of AAC-VIa. a) Hydrogen bonding interactions of the lower occupancy (occupancy = 0.19) gentamicin complex (cyan protein with gentamicin colored with gray carbon atoms). The higher occupancy gentamicin conformer (occupancy = 0.81) is shown with green carbon atoms. The C2′ substituent and the catalytic nucleophile (N3 amine) are circled in red and black, respectively. b) Hydrogen bonding interactions of the lower occupancy (occupancy = 0.39) tobramycin complex (cyan protein with tobramycin colored with green carbon atoms). The higher occupancy tobramycin conformer (occupancy = 0.61) is shown with grey carbon atoms. c) The AAC-Via-sisomicin complex (cyan protein carbon atoms with green sisomicin carbon atoms; hydrogen bonds are represented as black dashed lines) superimposed with the acetyl sisomicin product state (gray protein carbon atoms with gray sisomicin carbon atoms; hydrogen bonds are represented as red dashed lines). The primed ring which flips conformation upon acetylation of the central 2-deoxystreptamine ring is circled in red.

the gentamicin and tobramycin complexes, two differentially occupied conformers of the primed ring are present, whereas in the sisomicin, kanamycin A and B complexes only a single major conformer is present (Figure 2a, b and Figure S3). The primed ring of the kanamycin complexes and the higher occupancy conformers of tobramycin and gentamicin are in a similar conformation as the one in acetylated sisomicin product complex structure of AAC-VIa that was recently determined[13] (Figure 2 and Figure S3). These same studies on AAC-VIa showed that the conformation of the primed ring flips upon formation of the product state as a means to aid the release of the acetylated sisomicin product (Figure 2).[13] The lower occupancy gentamicin conformer matches the conformer found in the sisomicin complex instead. The primed ring is in the same conformation in both the tobramycin conformers but is rotated by the glycosidic bond by 107° in the lower occupancy conformer. This places the tobramycin C2′ amine deeper in the binding site towards the catalytic triad and the catalytic N3 amine nucleophile (Figure 2), in a manner similar to the lower occupancy gentamicin state. The distance of this C2′ group to the catalytic N3 nucleophile is variable in all of the structures, with a distance of 4.4 Å in the sisomicin complex, 4.9 Å and 4.4 Å in the gentamicin high and low occupancy conformers complexes, 5.2 Å in kanamycin A/B complexes, and 5.0 Å and 3.6 Å in the tobramycin high and low occupancy conformers complexes, respectively. In all aminoglycosides that get modified the C2′ substituent is an amine which can be positively charged, whereas a neutral hydroxyl is found in the catalytically inactive kanamycin A (Figure 1). Moreover, for the substrate that is turned over the poorest, the primed ring is found only in a conformation that mimics the product state, versus either a single catalytically competent conformer, or a mixture of conformers. The varied conformations of the primed ring, and in turn the localization of the C2′ substituent in direct proximity of the nucleophilic N3 amine of the catalytic triad alter the electrostatic environment of the active site in a substrate dependent manner.

Neutron crystal structures of AAC-VIa

The room temperature neutron crystal structures of AAC-VIa with gentamicin C1a and kanamycin B, which allow for visualization of protons at modest resolutions (< 2.6 Å), were determined (Table S2). A single conformer, corresponding to the higher occupancy conformers in the cryo-cooled X-ray crystal structures, is present (Figure 3a and c). In the previously determined neutron structure of AAC-VIa bound to sisomicin, a single hydrogen atom was observed in an LBHB in the catalytic triad formed between Glu192, His189 and the N3 amine of the antibiotic.[13] (Figure 3b). In the neutron crystal structure of AAC-VIa bound to gentamicin the distance between the Glu192 and His189 heavy atoms is 2.70 Å and the hydrogen atom is also found residing equidistant between heavy atoms in a canonical LBHB (Figure 3a). Moreover, the position of the hydrogen atom shifts from the standard distance of 1.0 Å, to 1.4 Å away from the His189 nitrogen (Figure 3). In the kanamycin B complex, the distance between heavy atoms is identical to the gentamicin complex, yet the hydrogen atom remains completely bound, and residing 1.0 Å from the nitrogen of His189, in what is a canonical hydrogen bond (Figure 3c). Coupled to the locating the position of the hydrogen atom from the omit density maps, the maximum coordinate error of the gentamicin (0.25 Å) and the kanamycin B (0.45 Å) complexes suggests the relevance of observed re-positioning of the His189 hydrogen atom in response to different substrates.

The difference in the location of this single hydrogen atom indicates the pK_a values of the hydrogen bond donor and acceptor atoms are not matched in the kanamycin B complex, but they are in the gentamicin and sisomicin antibiotic complexes. The position of this catalytic hydrogen atom (LBHB versus canonical hydrogen bond) correlates with the observed catalytic activity of AAC-VIa with these substrates, and the predicted enhancement of activity provided by an LBHB. Owing to the seemingly static nature of the AAC-VIa active site in the complexes determined with X-ray crystal-

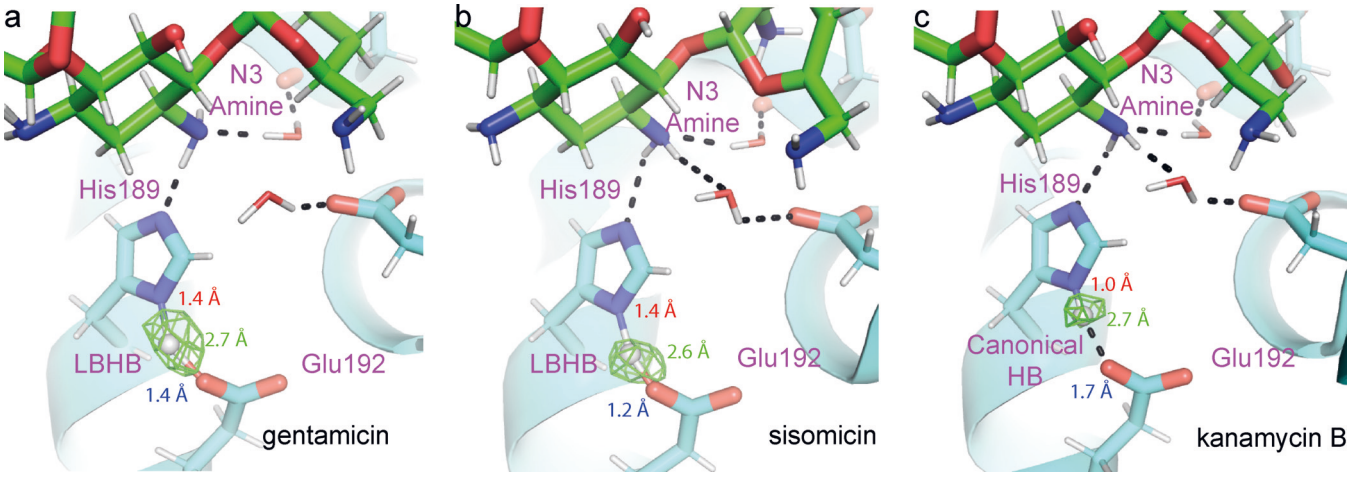

Figure 3. Neutron crystal structures of AAC-VIa. a) Gentamicin. b) Sisomicin. c) Kanamycin B. Hydrogen bonds observed in the nuclear density are shown as black dashed lines. The F_o-F_c nuclear omit density is shown for the hydrogen atom involved in the hydrogen bond between His189 and Glu192. The distances between heavy atoms (green text) and the distance of the His189 proton from the nitrogen (red text) and Glu192 oxygen (blue text) atoms are shown. The gentamicin, sisomicin and kanamycin B omit maps are contoured at 3.0, 2.8 and 3.0 σ, respectively.

lography, the modulation of this critical hydrogen bond is likely due to the electrostatics of the antibiotic substrates modulating the pKa values of the catalytic triad through the varied conformations of the antibiotic primed ring. We postulate that the ability of the enzyme to catalytically select antibiotics is directly related to the modulation of the hydrogen bond between catalytic residues in response to the placement of the C2′ substituent of the antibiotic in the proximity of the catalytic triad.

Molecular dynamics (MD) simulations of AAC-VIa complexes

Since the crystallographic structures of the AAC-VIa complexes only capture static snapshots of the enzyme, we were interested in understanding whether the dynamics of the antibiotic complexes were also modulated in response to the different substrates. The results of the 400 ns MD simulations indicate that sisomicin and gentamicin formed the most stable complexes (Figure 4), while kanamycin B formed a less stable complex that dissociated in less than 200 ns of the simulations (Figure S4). Interestingly, the kanamycin A simulations show tighter binding and stable interactions at this timescale, which is particularly intriguing as it is not a substrate of AAC-VIa (Figure S4). Tobramycin showed mixed behavior depending on the starting structures, with the higher occupancy conformer being more stable during the simulation (Figure S4). Comparison of the root mean square fluctuation (RMSF) values of the apoenzyme to the antibiotic-bound complexes revealed that binding of sisomicin to AAC-VIa lead to the protein becoming more rigid, while kanamycin B, the least efficiently turned over substrate, increased its conformational flexibility (Figure 4). Taken together, the simulations suggest protein dynamics play a role in the catalytic selection of antibiotics by AAC-VIa, in addition to the response of the protein to the electronic nature of substrates.

Discussion

The phenomenon of how the local electronic environment of enzyme active sites inherently tunes and facilitates biological catalysis is well known and documented in several different enzymes,[17] including members of the serine protease family of enzymes.[18] This is usually accomplished by altering the intrinsic pKa values of the functional groups involved, on both the enzymes as well as the substrates. The protonation states of enzyme functional groups are crucial for their ability to serve as electrophile, nucleophile or general acid–base catalysts. The resulting perturbed pK_a values can in turn influence the hydrogen bond distance and geometry, which can be utilized by the enzyme to kinetically distinguish between various substrates.[19]

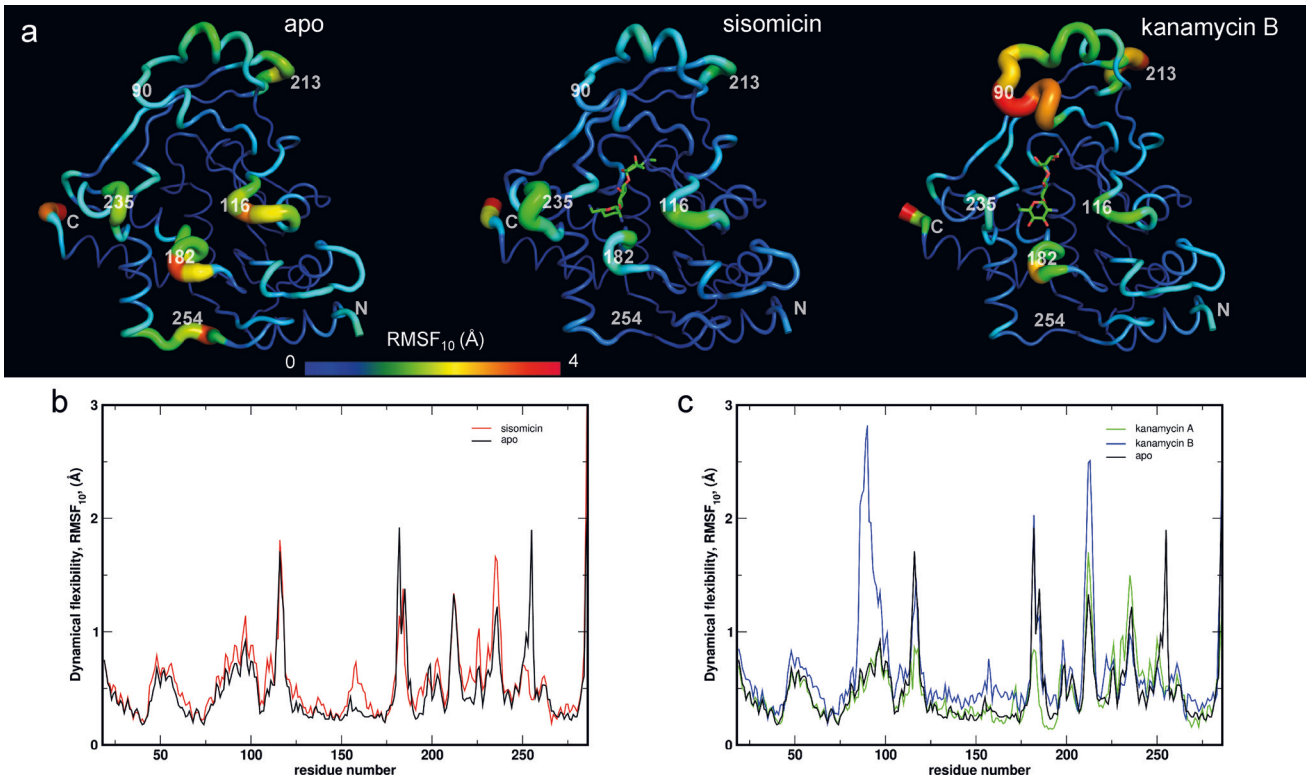

Figure 4. Change in protein flexibility upon antibiotic binding. a) Comparison of RMSF-10 between apoenzyme, and antibiotic bound complexes indicates that the protein shows decrease in flexibility in case of strongly binding antibiotic (sisomicin) and increase in protein flexibility in case of weaker binding antibiotic (kanamycin B). b) Quantitative comparison of RMSF-10 for apoenzyme, and sisomicin bound complex. c) Quantitative comparison of RMSF-10 for apoenzyme, kanamycin A and kanamycin B bound complexes. The scale ranges from 0–4 Å in panel (a) and has been adjusted to 0–3 Å in panels (b) and (c) for better comparison.

The organization and molecular interactions of the AAC-VIa active site is highly similar among all of the antibiotic complexes, which suggests that something more than molecular recognition is responsible for the observed specificity profile. This is not unique for aminoglycoside modifying enzymes; crystal structures of the aminoglycoside acetyltransferase(2′)-Ic with several antibiotics failed to provide explanation for differences in catalytic efficiencies with these substrates.[20] Like AAC-VIa, the aminoglycoside acetyltransferase-IIIb (AAC-IIIb) catalyzes the acetylation of the same antibiotic site and shares the same structural fold, but is highly promiscuous, modifying many structurally diverse aminoglycosides with higher turnover rates and similar catalytic efficiencies. Interestingly, similar to the differential kinetic behavior of AAC-VIa towards kanamycin B and A, binding of neomycin and paromomycin to AAC-IIIb leads to significant differences in protein dynamics as detected by hydrogen/deuterium exchange.[21] Additionally, the thermodynamics of ligand binding of these two antibiotics to AAC-IIIb occurs with opposite signs of heat capacity change (ΔCp).[22] Neomycin and paromomycin are structurally similar except for an amine group at the 6′ position in neomycin versus a hydroxyl group in paromomycin,[23] which clearly demonstrates a catalytic response of the protein to the electronic nature of the substrates.

In the case of AAC-VIa, the strongest effect on activity, but not binding, stems from the replacement of a single positively charged amine at the C2′ found in kanamycin B, versus a neutral hydroxyl in the catalytically inactive kanamycin A. This substitution completely abrogates detectable turnover in our assay conditions. The present X-ray crystallographic structural studies showed no obvious differences in the organization of the relatively static AAC-VIa active site that would explain the differences in substrate binding and kinetics. Rather the active site electrostatics, and in turn catalytic triad hydrogen bonding network is altered by the electrostatic environment provided by the substrate. Indeed, the conformation of the primed ring of these antibiotics varies significantly among the complexes, which suggests the altered electrostatic environment provided by the primed ring C2′ substituent is a determining factor in AAC-VIa catalytic activity. The C2′ amine is placed directly adjacent to the N3 nucleophile in the sisomicin and the lower occupancy gentamicin and tobramycin structures, yet it is the farthest from the nucleophile in the single kanamycin conformers.

Previous studies on AAC-VIa have also suggested that the replacement of a protonated C2′ amine with a neutral hydroxyl is a likely cause for the catalytic discrepancies observed for this enzyme.[15] Consistent with this, earlier work with different aminoglycoside modifying enzymes showed that the presence of an amine at this site affects catalytic activity[15] and the difference in binding enthalpy ($\Delta\Delta H = \Delta H_{\text{kanamycin A}} - \Delta H_{\text{kanamycin B}}$) can vary from -3.6 kcal mol^{-1} [24] to $+10.4$ kcal mol^{-1} [25] for different enzymes, which clearly demonstrates the underlying energetic basis of how this family of enzymes catalytically responds to the variable electronic nature of the antibiotic substrates.

Conclusion

The electrostatic modulation of a short hydrogen bond that is linked to AAC-VIa catalytic selection is a crucial piece of evidence in support of the role of low-barrier hydrogen bonds in enhancing catalysis. Occurrences of both LBHB and canonical hydrogen bonds in the same active site have been reported previously, although involving different residues.[12b] To our knowledge, this is the first report of both types of hydrogen bonds observed in the same active site involving the same residues and a direct demonstration of the catalytic enhancement provided by and proposed for LBHBs 30 years ago.

Experimental Section

AAC-VIa used for crystallography was expressed and purified as previously described.[15] Kinetic assays were carried out as previously described to ascertain that the enzyme is more than 95% active prior to flash freezing using liquid nitrogen and storing at -80 °C. Further experimental details are provided in the Supporting Information.

Accession codes: Structures and reflection data of AAC-VIa complexes reported here have been deposited to the Protein Data Bank under the accession codes: 6NP1, 6NP2, 6NP3, 6NP4, 6NP5, 6NTJ, 6NTI and 6O5U.

Acknowledgements

We thank Jaroslaw Majewski, Dean Myles and Andrey Kovalevsky for critical reading of the manuscript and valuable comments. This work was supported by grants from the National Science Foundation (MCB-1662080) and National Institute of General Medical Sciences (GM105978 to P.K.A.) and the Extreme Science and Engineering Discovery Environment (XSEDE), which is supported by National Science Foundation grant numbers MCB180199 and MCB190044. This work was also supported by St. Jude Children's Research Hospital (to T.M.), and American Lebanese Syrian Associated Charities (to T.M.). The ORNL Center for Structural Molecular Biology (FWP ERKP291) was supported by the Office of Biological and Environmental Research of the U.S. Department of Energy. Research at the SNS and High Flux Isotope Reactor of ORNL was sponsored by the Scientific User Facilities Division, Office of Basic Energy Sciences, U.S. Department of Energy. This research used resources of the Advanced Photon Source (APS), a U.S. Department of Energy Office of Science User Facility operated for the DOE Office of Science by Argonne National Laboratory under Contract No. DE-AC02-06CH11357. GM/CA at the APS has been funded in whole or in part with Federal funds from the National Cancer Institute (ACB-12002) and the National Institute of General Medical Sciences (AGM-12006).

Conflict of interest

The authors declare no conflict of interest.

Keywords: antibiotic resistance · enzyme catalysis · low-barrier hydrogen bond · neutron diffraction · X-ray diffraction

How to cite: *Angew. Chem. Int. Ed.* **2019**, *58*, 16260–16266
Angew. Chem. **2019**, *131*, 16406–16412

[1] A. E. Todd, C. A. Orengo, J. M. Thornton, *Trends Biochem. Sci.* **2002**, *27*, 419–426.
[2] a) D. Ringe, G. A. Petsko, *Science* **2008**, *320*, 1428–1429; b) A. Warshel, *J. Biol. Chem.* **1998**, *273*, 27035–27038.
[3] J. A. Gerlt, P. G. Gassman, *J. Am. Chem. Soc.* **1993**, *115*, 11552.
[4] P. A. Frey, S. A. Whitt, J. B. Tobin, *Science* **1994**, *264*, 1927–1930.
[5] Z. T. Gu, D. G. Drueckhammer, L. Kurz, K. Liu, D. P. Martin, A. McDermott, *Biochemistry* **1999**, *38*, 8022–8031.
[6] J. L. Markley, W. M. Westler, *Biochemistry* **1996**, *35*, 11092–11097.
[7] Q. J. Zhao, C. Abeygunawardana, A. G. Gittis, A. S. Mildvan, *Biochemistry* **1997**, *36*, 14616–14626.
[8] S. Dajnowicz, J. M. Parks, X. Hu, K. Gesler, A. Y. Kovalevsky, T. C. Mueser, *J. Biol. Chem.* **2017**, *292*, 5970–5980.
[9] W. W. Cleland, P. A. Frey, J. A. Gerlt, *J. Biol. Chem.* **1998**, *273*, 25529–25532.
[10] W. W. Cleland, M. M. Kreevoy, *Science* **1994**, *264*, 1887–1890.
[11] a) C. N. Schutz, A. Warshel, *Proteins Struct. Funct. Bioinf.* **2004**, *55*, 711–723; b) A. Warshel, A. Papazyan, P. A. Kollman, *Science* **1995**, *269*, 102–106; c) J. P. Guthrie, *Chem. Biol.* **1996**, *3*, 163–170; d) T. Tamada, T. Kinoshita, K. Kurihara, M. Adachi, T. Ohhara, K. Imai, R. Kuroki, T. Tada, *J. Am. Chem. Soc.* **2009**, *131*, 11033–11040.
[12] a) C. N. Fuhrmann, M. D. Daugherty, D. A. Agard, *J. Am. Chem. Soc.* **2006**, *128*, 9086–9102; b) A. Das, S. Mahale, V. Prashar, S. Bihani, J. L. Ferrer, M. V. Hosur, *J. Am. Chem. Soc.* **2010**, *132*, 6366–6373.
[13] P. Kumar, E. H. Serpersu, M. J. Cuneo, *Sci. Adv.* **2018**, *4*, eaas8667.
[14] P. Kumar, B. Selvaraj, E. H. Serpersu, M. J. Cuneo, *J. Med. Chem.* **2018**, *61*, 10218–10227.
[15] P. Kumar, E. H. Serpersu, *Proteins Struct. Funct. Bioinf.* **2017**, *85*, 1258–1265.
[16] J. Schiebel, R. Gaspari, A. Sandner, K. Ngo, H. D. Gerber, A. Cavalli, A. Ostermann, A. Heine, G. Klebe, *Angew. Chem. Int. Ed.* **2017**, *56*, 4887–4890; *Angew. Chem.* **2017**, *129*, 4965–4969.
[17] a) M. Schubert, D. K. Poon, J. Wicki, C. A. Tarling, E. M. Kwan, J. E. Nielsen, S. G. Withers, L. P. McIntosh, *Biochemistry* **2007**, *46*, 7383–7395; b) M. J. Plantinga, A. V. Korennykh, J. A. Piccirilli, C. C. Correll, *Biochemistry* **2008**, *47*, 8912–8918; c) M. F. Perutz, *Science* **1978**, *201*, 1187–1191.
[18] J. Batra, A. Szabo, T. R. Caulfield, A. S. Soares, M. Sahin-Toth, E. S. Radisky, *J. Biol. Chem.* **2013**, *288*, 9848–9859.
[19] T. K. Harris, G. J. Turner, *IUBMB Life* **2002**, *53*, 85–98.
[20] M. W. Vetting, S. S. Hegde, F. Javid-Majd, J. S. Blanchard, S. L. Roderick, *Nat. Struct. Mol. Biol.* **2002**, *9*, 653.
[21] A. L. Norris, J. Nickels, A. P. Sokolov, E. H. Serpersu, *Biochemistry* **2014**, *53*, 30–38.
[22] A. L. Norris, E. H. Serpersu, *Biochemistry* **2010**, *49*, 4036–4042.
[23] A. L. Norris, C. Ozen, E. H. Serpersu, *Biochemistry* **2010**, *49*, 4027–4035.
[24] C. Özen, E. H. Serpersu, *Biochemistry* **2004**, *43*, 14667–14675.
[25] A. L. Norris, E. H. Serpersu, *Protein Sci.* **2013**, *22*, 916–928.

Manuscript received: July 9, 2019
Revised manuscript received: September 11, 2019
Accepted manuscript online: September 13, 2019
Version of record online: September 24, 2019

